



Published in final edited form as:

*Hypertension*. 2010 February ; 55(2): 555–561. doi:10.1161/HYPERTENSIONAHA.109.142505.

## NEOINTIMAL HYPERPLASIA AND VASOREACTIVITY ARE CONTROLLED BY GENETIC ELEMENTS ON RAT CHROMOSOME 3

Andrea L. Nestor Kalinoski<sup>1</sup>, Ramona S. Ramdath<sup>1</sup>, Kay M. Langenderfer<sup>1</sup>, Saad Sikanderkhel<sup>1</sup>, Sarah DeRaedt<sup>1</sup>, Marlene Welch<sup>1</sup>, James L. Park<sup>2</sup>, Timothy Pringle<sup>1</sup>, Bina Joe<sup>3</sup>, George T. Cicila<sup>3</sup>, and David C. Allison<sup>1,3</sup>

<sup>1</sup>Department of Surgery and The University of Toledo Advanced Microscopy & Imaging Center, Toledo, Ohio 43614, USA

<sup>2</sup>Department of Nephrology, The University of Michigan, Ann Arbor, MI 48109

<sup>3</sup>Department of Physiology and Pharmacology, The University of Toledo, College of Medicine, 3000 Arlington Ave., Toledo, Ohio 43614, USA

### Abstract

Neointimal Hyperplasia (NIH) can lead to restenosis after clinical vascular interventions. NIH results from complex, and poorly understood, interactions between signaling cascades in the extracellular matrix and disrupted endothelium which leads to vessel occlusion. Quantitative Trait Loci (QTLs) were previously reported on rat chromosomes 3 and 6 through linkage analysis of post-injury NIH in mid-iliac arterial sections. In the current study, substitution mapping validated the RNO3 NIH QTL but not the RNO6 NIH QTL. The SHR.BN3 congenic strain had a three-fold increase in %NIH compared to the parental SHR strain. A double congenic study of RNO3+RNO6 NIH QTL segments suggested less than additive effects of these two genomic regions. To test the hypothesis that changes in vessel dynamics account for the differences in NIH formation, we performed vascular reactivity studies in the BN, SHR, SHR.BN3 and SHR.BN6 strains. De-endothelialized left common carotid artery rings of the SHR.BN3 showed an increased vascular responsiveness when treated with serotonin or prostaglandin F<sub>2α</sub>, with significant differences in EC<sub>50</sub> and E<sub>max</sub> ( $p < 0.01$ ) values compared to the SHR parental strain. Since both vascular reactivity and %NIH formation in the SHR.BN3 strain are significantly higher than the SHR strain, we postulate that these traits may be associated and are controlled by genetic elements on RNO3. In summary, these results confirm that the RNO3 NIH QTL carries the gene(s) contributing to post-injury NIH formation.

### Keywords

Neointimal Hyperplasia; QTL; Congenics; Rat; Vascular Reactivity

---

\*Correspondence: Andrea Nestor Kalinoski, Ph.D., Department of Surgery, The University of Toledo College of Medicine, 3000 Arlington Ave., Mailstop 1000, Toledo, Ohio 43614-5804, Phone: 419-383-4205, Fax: 419-383-6230, andrea.kalinoski@utoledo.edu.

**Disclosures**  
None

## Introduction

Cardiovascular interventions such as arterial grafts, stents, and balloon angioplasties often fail because of recurrent vascular stenosis due to the development of neointimal hyperplasia (NIH). NIH adversely affects patient outcome following vascular interventions. For example, restenosis following clinical interventions in the vascular system occurs in upwards of 37% of patients after balloon angioplasty for coronary artery disease<sup>1-3</sup> and in 20% of patients who have undergone carotid endarterectomy.<sup>4</sup> Furthermore, there is a 10% yearly failure rate for grafts in the coronary and peripheral arterial systems<sup>5-7</sup> with NIH being the major contributing factor.

Currently, there are no effective medical therapies to prevent or treat NIH. A need for more specific therapies is underscored by the failure of clinical trials evaluating the empiric use of aspirin, heparin and calcium channel blockers<sup>1, 8</sup> to prevent restenosis after vascular interventions. Furthermore, the use of drug eluting stents to prevent NIH is currently being closely examined because of the additional risk of drug toxicity without any observed increase in long term efficacy compared to normal stents.<sup>9-11</sup> The lack of effective therapies to prevent or medically treat NIH following vascular procedures may be due, in part, to a poor understanding of the mechanisms underlying vascular remodeling following cardiovascular interventions. Previously, we obtained evidence for genetic factors governing NIH. Differences in NIH-injury response of the left common and external iliac artery were observed among inbred strains of rats<sup>2</sup> and a subsequent genome scan of a segregating F<sub>2</sub> (SHR X BN) population phenotyped for postinjury NIH formation and vascular wall differences identified possible NIH-related QTLs on rat chromosomes 3 and 6 (RNO3 and RNO6).<sup>12</sup> The current report constitutes a continuation of this project with the long-term goal to identify the gene(s) controlling vascular remodeling and restenosis after injury. We now confirm the presence of an NIH QTL on RNO3 containing the allele(s) in part responsible for controlling the strain differences in the formation of injury-induced NIH. Unexpectedly, this newly developed RNO3 congenic rat strain also provided evidence for eliciting genetic control of vasoreactivity.

## Methods

### Rat Strains

Inbred Spontaneously Hypertensive Rats (SHR/NHsd) and Brown Norway (BN/SsNHsd) rat strains (obtained from Harlan Sprague-Dawley, Indianapolis, IN) were used to establish colonies that were maintained in the Division of Laboratory Animal Resources at The University of Toledo Health Science Campus (UTHSC). Hereafter, these inbred strains will be referred to as SHR and BN, respectively. The previous genome scan of an F<sub>2</sub> (SHR x BN) population<sup>12</sup> and the present substitution mapping were conducted using the same SHR and BN colonies. Breeding programs were approved by the Institutional Animal Care and Use Committee and complied with the National Institutes of Health "Guide for the Care and Use of Laboratory Animals". All rats were housed with the appropriate temperature and humidity controls with 12 hour light/dark cycles and maintained on standard rat chow (Ralston Purina, Diet 5001) with *ad libitum* access to water.

Congenic strains were developed using a marker-assisted, speed congenic approach<sup>13</sup> on the SHR strain as the background and the BN strain as the donor strain. The breeding paradigm was as follows: male F<sub>1</sub> rats, bred by crossing male BN rats with female SHR rats, were backcrossed to female SHR rats. In general, male progeny heterozygous for the RNO3 and RNO6 NIH QTL-containing regions (loci genotyped are described below for each congenic strain) and containing the fewest number of BN-rat alleles at the other loci in the genome were selected for backcrossing to female SHR rats. After the first backcross generation,

SHR.BN3 and SHR.BN6 congenic strains were developed independently. For each generation, the male rat heterozygous for all markers in the NIH QTL-containing region and carrying the fewest BNrat alleles in the remainder of the genome was bred with up to 8 female SHR rats. In one generation, a female RNO3 backcross rat was bred with a male SHR, thus the RNO3 and double congenic strain carry the SHR Y chromosome. However, the RNO6 congenic carries the BN Y chromosome.

Five backcross generations were required to breed the congenic strains. Male and female rats heterozygous for the RNO3 or RNO6 NIH QTL-containing regions and lacking BN-rat alleles in the background were then mated to fix the BN-rat alleles in the congenic regions and SHR-rat alleles outside of the congenic segment and on all other chromosomes. Brother-sister mating was subsequently used to maintain congenic rat strains. The “double” congenic strain was similarly bred by crossing female SHR.BN6 and male SHR.BN3 congenic strains and selecting rats heterozygous for both the RNO3 and RNO6 QTL-containing regions in the F<sub>1</sub> progeny. Male and female rats heterozygous for both congenic regions were then mated to fix BN-alleles in the congenic regions, and brother-sister mating was subsequently used to maintain the strain. Hereafter, this congenic strain will be referred to as SHR.BN (3+6).

### Vascular Injury

Male rats 10–12 weeks of age (~300g) underwent a standard balloon vascular injury as previously described.<sup>2, 12</sup> Briefly, rats were sedated with 2% isoflurane by O<sub>2</sub> inhalation and anesthetized intraperitoneally with 80 mg/kg ketamine and 12 mg/kg xylazine. A sterile field was established and the left femoral artery was isolated, dilated (2% lidocaine) and cannulated with a 2-Fr balloon catheter. The catheter was advanced to the distal aorta, inflated to 0.1ml with normal saline and retracted three times to denude the endothelial layer of the common and external iliac artery. This injury may also damage the media of the vessel. The left femoral artery was tied off and the skin closed with an absorbable suture.

### Fixation and Preparation of Mid-iliac Artery Sections

Eight weeks post-injury rats were anesthetized as above and perfused with PBS, followed by 10% neutral buffered formalin as previously described.<sup>2</sup> Iliac arteries were extracted, embedded in 5% agarose and processed for embedding in paraffin. Injured and uninjured contralateral control mid-iliac arteries were cut to 5µm thick sections and stained using Verhoeff-Van Gieson for elastin.<sup>2</sup>

### Genotyping

Microsatellite loci were genotyped by PCR amplification as previously described.<sup>12</sup> Genomic DNA was prepared from the parental SHR, BN and congenic strains by tail biopsy using a DNeasy 96 well kit (Qiagen, Valencia, CA). PCR products were electrophoretically size-fractionated on 3:1 high resolution blend agarose (Amresco, Solon, OH) or 4% Metaphor agarose gels (Cambrex Bio Science, Walkersville, MD) and visualized with ethidium bromide staining.

### Vessel Measurements

Image analysis measurements of the media area, neointimal area, and internal elastic lamina (IEL) length were made on the injured and uninjured contralateral control iliac arteries of the BN, SHR and congenic strains with Scion Image (Frederick, Maryland). These measurements were used to calculate the media width, circular area ( $IEL^2/4\pi$ ), lumen size and total arterial area due to NIH (designated as percent NIH, %NIH) of each vessel as previously described.<sup>12</sup> All measurements are reported as mean ± % coefficient of variation,

$\%CV = (\text{standard deviation/mean}) \times 100$ . Body-weight adjusted heart-weight was also calculated by adjusting heart-weight for differences in body-weight using the regression of heartweight on body-weight for each animal.<sup>14, 15</sup>

The parameters calculated related to vascular injury included: injured vessel circular area, media area, media width, NIH area, media area + NIH area, lumen size, and %NIH. The uninjured contralateral control vessel parameters, not related to the vascular injury, included uninjured control vessel circular area, media area and media width. All statistical analyses were conducted as previously reported.<sup>12</sup>

### Rats for Vasoreactivity

Male parental and congenic rats (11–12 weeks old) were bred in our colony at the UTHSC and shipped to the University of Michigan for reactivity experiments. All rats were maintained on normal chow in specific pathogen-free facilities. The reactivity procedures performed with the rats were in accordance with guidelines of the University of Michigan Committee on the use and care of animals. The University of Michigan Unit for Laboratory Animal Medicine provided veterinary care. The animal care and use program also conformed to the standards set in “The Guide for the Care and Use of laboratory Animals.”

### Vascular Reactivity Experiments

Left common carotid arteries were cut into rings (3 mm in length), and the endothelium was removed by perfusing the ring lumen with 100  $\mu\text{L}$  of 0.1 Triton-X 100 in PBS. Carotid rings were mounted in a myograph system (DMT-USA, Inc., Marietta, GA) and bathed with warmed (37°C), aerated (95% O<sub>2</sub>/5% CO<sub>2</sub>) physiological salt solution (PSS, mmol/L: NaCl 130, KCl 4.7, KHPO<sub>4</sub> 1.18, MgSO<sub>4</sub> 1.17, CaCl<sub>2</sub> 1.6, NaHCO<sub>3</sub> 14.9, dextrose 5.5, CaNa<sub>2</sub> EDTA 0.03). Carotid artery rings were set at 1.5 g passive tension and equilibrated for 1 hr. with washes every 20 min. Prior to determination of concentration response curves, the rings were subjected to a “wake-up” protocol consisting of two consecutive contractions with isotonic high-K<sup>+</sup>-containing physiological salt solution (KPSS) (mmol/L: NaCl 14.7, KCl 100, KHPO<sub>4</sub> 1.18, MgSO<sub>4</sub> 1.17, CaCl<sub>2</sub> 1.6, NaHCO<sub>3</sub> 14.9, dextrose 5.5, CaNa<sub>2</sub> EDTA 0.03), followed by a contraction with phenylephrine (PE; 10<sup>-7</sup> mol/L). After the wake-up protocol, serotonin (5HT; Sigma Chemical company, St. Louis, MO, 10<sup>-9</sup> mol/L to 10<sup>-4</sup> mol/L) and PGF<sub>2 $\alpha$</sub>  (Cayman Chemical, Ann Arbor, MI, 10<sup>-9</sup> mol/L to 3 $\times$ 10<sup>-5</sup> mol/L) concentration responses were performed in the endothelium-denuded rings. Both concentration responses were performed in each of the rings, but the order of the agonists was randomized on each day the experiments were performed.<sup>16</sup>

### Vasoreactivity Data and Statistical Analysis

Agonist EC<sub>50</sub> values were calculated with a nonlinear regression analysis with the algorithm [effect = maximum response/1 + (EC<sub>50</sub>/agonist concentration)] in the computer program Graph Pad Prism (San Diego, CA). Data are expressed as mean  $\pm$  SEM, and concentration-response data were analyzed using one-way ANOVA followed by a Bonferroni post-hoc test. Differences in EC<sub>50</sub> values were evaluated using one-way ANOVA with a Bonferroni post-hoc test ( $p < 0.05$ ).

## Results

### Extent of the regions introgressed in the congenic SHR.BN3, SHR.BN6 and SHR.BN (3+6) strains

Physical maps summarizing the regions of BN RNO3 and RNO6 introgressed into the SHR genetic background are presented in Fig. 1. The SHR.BN3 strain carries a 50.6 Mb region of the BN-rat RNO3 q-terminus, between *D3Rat159* and *D3Rat1* (Fig. 1). The SHR.BN6 strain

carries a 45.5 Mb region of RNO6, between markers *D6Rat40* and *D6Rat170* (Fig. 1). The “double congenic” strain incorporated both regions of RNO3 and RNO6 from the BN strain introgressed into the SHR genetic background and will be referred to as SHR.BN (3+6).

### Injured Vessel Analysis

Table 1 shows the injured vessel parameters measured for the parental SHR compared with those of the SHR.BN3 and SHR.BN6 congenic rat strains. The injured vessels of the SHR.BN3, which carry high injury-induced NIH QTL allele(s), showed significant increases in %NIH ( $p = 0.001$ ) and NIH area ( $p = 0.002$ ) compared to the parental SHR strain (Fig. 2A–B, Table 1). Specifically, a 3-fold higher %NIH developed 8 weeks post-injury in the SHR.BN3 congenic strain (28.31%, Table 1, Fig. 2B) as compared to the parental, SHR strain (9.63%, Table 1, Fig. 2A). Although not significant, the increase in NIH area in the injured SHR.BN3 vessels was associated with a decrease in the media area of these vessels when compared to the injured SHR vessels ( $p = \text{NS}$ , Table 1, Fig. 2). There was also a slight increase in circular area compared with injured SHR vessels ( $p = \text{NS}$ , Table 1, Fig. 2). Thus, the injured SHR.BN3 vessels did not show a significant post-injury dilation. In contrast, the SHR.BN6 congenic strain, carrying a possible high %NIH QTL and the QTL(s) associated with low media area and media width in uninjured control vessels<sup>12</sup>, did not develop a significant increase in NIH compared to the parental SHR strain (Table 1, Fig. 2C). However, significantly higher circular area and lumen size were observed in injured SHR.BN6 vessels, compared to injured SHR vessels ( $p < 0.01$ , Table 1, Fig. 2C), a finding consistent with a lack of injury induced vasoconstriction occurring in these vessels.

### Uninjured Contralateral Control Vessel Analysis

Table 2 shows a comparison of the parameters measured for the uninjured control vessels of the parental SHR and congenic SHR.BN3 and SHR.BN6 strains harvested 8 weeks after vascular injury. The same parameters were measured in the uninjured contralateral control SHR and congenic strain iliac arteries as in the initial  $F_2$  (SHR X BN) genome scan,<sup>12</sup> including circular area, media area, media width and lumen size. In contrast to the injured vessel analysis, no significant differences were observed in the uninjured control vessel measurements of the parental SHR strain compared to either congenic strain. Although there were no significant differences in the SHR.BN3 and SHR uninjured control vessel measurements, each measured parameter was smaller in the SHR.BN3 congenic strain than the parental SHR and SHR.BN6 congenic strains (Table 2).

However, significant differences were observed between the SHR.BN3 and SHR.BN6 congenic strains for the following uninjured, control vessel parameters: circular area ( $p = 0.0076$ ), media area ( $p = 0.0036$ ) and media width ( $p = 0.0032$ ) (Table 2). These differences were possibly due to the uninjured control vessel QTLs for media area and media width previously found on RNO6<sup>12</sup> (Table 2).

### Comparison of Uninjured Control vs. Injured Vessel Measurements within Strains

A comparison of uninjured control and injured vessel parameters for each of the three rat strains is shown in Table S1 please see <http://hyper.ahajournals.org>. A significant decrease was found in the lumen size of the uninjured control vessels compared to the injured vessels of the parental SHR strain ( $p = 0.0045$ , Table S1 please see <http://hyper.ahajournals.org>). The results observed for the congenic SHR.BN6 strain ( $N = 25$ ) were similar to the parental SHR strain, with significantly smaller injured vessel media area ( $p = 0.0005$ ) and media width ( $p = 0.0013$ ) compared to those of uninjured control vessels (Table S1 please see <http://hyper.ahajournals.org>). There were no significant differences in the circular area, lumen size, media area or media width of the uninjured control and injured vessels of the SHR.BN3 strain (Table S1 please see <http://hyper.ahajournals.org>).

## “Double Congenic” Vessel Analysis

Table S2 please see <http://hyper.ahajournals.org> summarizes the vessel parameters measured in a separate experiment comparing the parental, SHR strain with the double congenic strain SHR.BN (3+6) which carries both the RNO3 and RNO6 QTL containing regions. The double congenic and the SHR.BN6 rats were similar in that the vessels of both strains had significantly lower media area ( $p = 0.0430$ ), media width ( $p = 0.0163$ ) and lumen size ( $p = 0.0359$ ) in injured vessels when compared to uninjured control vessels (Table S2 please see <http://hyper.ahajournals.org>, Fig. 2D). Injured vessel parameters of the SHR and double congenic rats, were as expected, significantly different in %NIH ( $p = 0.0269$ ), NIH Area ( $p = 0.0223$ ), media area ( $p = 0.0157$ ) and media width ( $p = 0.0125$ ) (Table S2 please see <http://hyper.ahajournals.org>). These results suggest that the two %NIH QTL-containing regions [RNO3 (%NIH, 28.31, Table 1, Fig. 2B) and RNO6 (%NIH, 12.60, Table 1, Fig. 2C)] showed less than additive effects in the double congenic strain (%NIH, 23.76, Table S2 please see <http://hyper.ahajournals.org>), possibly due to differences in media area and media width.

## Vascular Reactivity Experiments

Vascular reactivity was studied to further characterize phenotypes potentially linked to the observed NIH response. Figure 3 shows the results of reactivity experiments performed on the parental (BN and SHR) and congenic (SHR.BN3 and SHR.BN6) rat strains with two different agonists. Concentration response curves were generated (Fig. 3) in endothelium-denuded carotid artery rings with increasing concentrations of prostaglandin F<sub>2α</sub> (PGF<sub>2α</sub>) and serotonin (5HT). We compared the vasopressor response of the individual congenic strains to both the SHR and BN strains at each concentration. PGF<sub>2α</sub> caused a concentration-dependent contraction in the endothelium denuded rings from each of the rat strains. The SHR.BN3 congenic strain showed significantly higher sensitivity ( $EC_{50} = 6.54 \pm 0.14$ ) to increasing concentrations of PGF<sub>2α</sub> compared to the parental SHR and BN strains ( $EC_{50} = 5.74 \pm 0.04$  and  $5.57 \pm 0.03$ , respectively) in the concentration response curve (Fig. 3). Furthermore, we observed a significant increase in PGF<sub>2α</sub>  $E_{max}$  for the SHR, SHR.BN3 and SHR.BN6 strains ( $E_{max}$  152.05, 154.20 and 157.04, respectively) compared to the BN strain ( $E_{max} = 102.75$ ,  $p < 0.05$ , Fig. 3A).

The SHR.BN3 congenic strain also showed a concentration-dependent response to 5HT (Fig. 3B) that was similar to that observed for PGF<sub>2α</sub> (Fig. 3A), although with a slightly higher  $EC_{50}$  ( $6.66 \pm 0.05$ ) and a slightly decreased  $E_{max}$  ( $139.10 \pm 0.03$ , Fig. 3). The SHR.BN3 rats showed a significantly different concentration response profile to 5HT compared to both the SHR and BN strains (Fig. 3B,  $p < 0.05$ ). Most notably, the  $EC_{50}$  for the SHR.BN3 5HT concentration response curve showed a leftward shift, compared to those of the SHR.BN6, SHR, and BN strains (Fig. 3B). Interestingly, the parental BN strain was the least sensitive strain at comparable  $EC_{50}$  and  $E_{max}$  values for both PGF<sub>2α</sub> and 5HT (Fig. 3). The SHR.BN3 congenic strain was clearly the most sensitive to both agonists and showed a concentration-dependent vasoreactivity within the endothelium-denuded aortic rings, confirming an increased vasoreactivity of SHR.BN3 congenic rats when compared to the parental SHR and BN strains.

## Discussion

The primary goal of this study was to corroborate the putative NIH QTLs identified in the initial F<sub>2</sub> (SHR X BN) genome scan<sup>12</sup> and to delimit the chromosomal region containing the gene(s) responsible for post-injury NIH formation. Congenic strains were generated to introgress the NIH QTLs identified on RNO3 and RNO6. The phenotypic data shown in Table 1 from these newly developed congenic strains validates the existence of an NIH QTL

on RNO3. The identification of the RNO3 interval associated with differences in NIH constitutes an important step in the genetic dissection of the NIH QTL, with the SHR.BN3 congenic strain serving as a substrate for further substitution mapping.

The second goal of our study was to optimize the morphological parameters to be measured by which the genetic determinants of NIH should be followed by substitution mapping. There were no significant differences between the SHR parental strain and either of the congenic strains in any of the measured, uninjured control vessel parameters (Table 2). This finding leads us to conclude that future mapping studies should be conducted exclusively after vessel injury, as this is the only condition wherein QTL effects are observable between SHR, SHR.BN3 and SHR.BN(3+6) strains (Table 1).

The third objective of the study was to identify associated phenotypes of NIH that may help us gain insight into the underlying mechanisms involved in intimal thickening. Intriguingly, upon catheter insertion, we observed marked differences in vascular resistance between the individual parental and congenic strains (data not shown), suggesting that differences in vascular reactivity and the media elastin layers may contribute to the observed differences in NIH between the two strains (Table 1). The finding of elevated vasoconstriction in the SHR vessels compared to BN vessels in response to 5HT and higher concentrations of PGF<sub>2α</sub> (Fig. 3) lend support to the idea that alterations in vessel wall dynamics may contribute to NIH formation in response to injury. It is interesting that the RNO3 alleles from the BN-rat introgressed into the SHR.BN3 congenic strain led to a rapid and sustained vasoconstriction when compared to that observed in the parental SHR vessels (Fig. 3) and this vasoconstrictive response segregated with the marked increase in %NIH (Table 1, Fig. 2). Thus, the SHR.BN3 congenic strain should provide a foundation to generate newer iterations of congenic substrains to test for possible relationships between these NIH and vasoconstrictive phenotypes.

The RNO6 NIH QTL identified in our previous F<sub>2</sub> genome scan<sup>12</sup> was not confirmed by substitution mapping. This was perhaps to be expected because the RNO6 NIH QTL reached only suggestive LOD scores for all parameters measured (i.e., %NIH, media area and media width) in the previous linkage analysis.<sup>12</sup> This also means that the net effects of BN-rat RNO6 alleles substituted do not account for differences in NIH observed at this locus in the F<sub>2</sub> (SHR X BN) population.<sup>12</sup> The negative result of lack of corroboration with a congenic strain however does not necessarily mean that an NIH QTL does not exist on RNO6. Similar to the identification of multiple opposing blood pressure QTLs on RNO10 and RNO8<sup>17, 18</sup>, it is also possible that the congenic segment of SHR.BN6 contains closely-linked multiple NIH QTLs having opposing effects. Further genetic dissection using the SHR.BN6 congenic strain will be required to resolve this possibility.

In conclusion, we have clearly validated the existence of an RNO3 NIH QTL by congenic strain analysis. Considering that the region mapped requires further high resolution mapping, a list of annotated candidate genes is not particularly relevant or useful to add to this report at the present time. Preparations are currently underway for further fine mapping of the RNO3 NIH QTL using the SHR.BN3 congenic strain. Refining the limits of the RNO3 NIH QTL containing region should facilitate identification of pertinent genetic elements responsible for the development of NIH, and may improve our understanding of the mechanisms underlying restenosis.

## Supplementary Material

Refer to Web version on PubMed Central for supplementary material.

## Acknowledgments

### Sources of Funding

This work was supported by The University of Toledo Foundation, Cancer Biology Research Fund. Funding from the NIH to GTC (HL68994) and BJ (HL076709 & HL020176) are gratefully acknowledged.

## References

1. Liu MW, Roubin GS, King SB 3rd. Restenosis after coronary angioplasty. Potential biologic determinants and role of intimal hyperplasia. *Circulation*. 1989; 79:1374–1387. [PubMed: 2524293]
2. Assadnia S, Rapp JP, Nestor AL, Pringle T, Cerilli GJ, Gunning WT III, Webb TH, Kligman M, Allison DC. Strain Differences in Neointimal Hyperplasia in the Rat. *Circ Res*. 1999; 84:1252–1257. [PubMed: 10364562]
3. Sadideen H, Taylor PR, Padayachee TS. Restenosis after Carotid Endarterectomy. *International Journal of Clinical Practice*. 2006; 60:1625–1630. [PubMed: 16669835]
4. Healy DA, Zierler RE, Nicholls SC, Clowes AW, Primozich JF, Bergelin RO, Strandness DE Jr. Long-term follow-up and clinical outcome of carotid restenosis. *J Vasc Surg*. 1989; 10:662–668. [PubMed: 2585655]
5. Bulkley BH, Hutchins GM Accelerated “atherosclerosis”. A morphologic study of 97 saphenous vein coronary artery bypass grafts. *Circulation*. 1977; 55:163–169. [PubMed: 299723]
6. Echave V, Koornick AR, Haimov M, Jacobson JH 2nd. Intimal hyperplasia as a complication of the use of the polytetrafluoroethylene graft for femoral-popliteal bypass. *Surgery*. 1979; 86:791–798. [PubMed: 515948]
7. Imparato AM, Bracco A, Kim GE, Zeff R. Intimal and neointimal fibrous proliferation causing failure of arterial reconstructions. *Surgery*. 1972; 72:1007–1017. [PubMed: 5087270]
8. Nunes GL, Sgoutas DS, Redden RA, Sigman SR, Gravanis MB, King SB 3rd, Berk BC. Combination of vitamins C and E alters the response to coronary balloon injury in the pig. *Arterioscler Thromb Vasc Biol*. 1995; 15:156–165. [PubMed: 7749812]
9. Kuchulakanti P, Waksman R. Therapeutic potential of oral antiproliferative agents in the prevention of coronary restenosis. *Drugs*. 2004; 64:2379–2388. [PubMed: 15481997]
10. Marzocchi A, Saia F, Piovaccari G, Manari A, Aurier E, Benassi A, Cremonesi A, Percoco G, Varani E, Magnavacchi P, Guastaroba P, Grilli R, Maresta A. Long-term safety and efficacy of drug-eluting stents: two-year results of the REAL (REGistro AngiopLastiche dell’Emilia Romagna) multicenter registry. *Circulation*. 2007; 115:3181–3188. [PubMed: 17562952]
11. Pfisterer M, Brunner-La Rocca HP, Buser PT, Rickenbacher P, Hunziker P, Mueller C, Jeger R, Bader F, Osswald S, Kaiser C. Late clinical events after clopidogrel discontinuation may limit the benefit of drug-eluting stents: an observational study of drug-eluting versus bare-metal stents. *J Am Coll Cardiol*. 2006; 48:2584–2591. [PubMed: 17174201]
12. Nestor AL, Cicila GT, Karol SE, Langenderfer KM, Hollopeter SL, Allison DC. Linkage analysis of neointimal hyperplasia and vascular wall transformation after balloon angioplasty. *Physiol Genomics*. 2006; 25:286–293. [PubMed: 16434542]
13. Wakeland E, Morel L, Achey K, Yui M, Longmate J. Speed congenics: a classic technique in the fast lane (relatively speaking). *Immunol Today*. 1997; 18:472–477. [PubMed: 9357138]
14. Garrett MR, Dene H, Walder R, Zhang QY, Cicila GT, Assadnia S, Deng AY, Rapp JP. Genome scan and congenic strains for blood pressure QTL using Dahl salt-sensitive rats. *Genome Res*. 1998; 8:711–723. [PubMed: 9685318]
15. Cicila GT, Choi C, Dene H, Lee SJ, Rapp JP. Two blood pressure/cardiac mass quantitative trait loci on chromosome 3 in Dahl rats. *Mamm Genome*. 1999; 10:112–116. [PubMed: 9922389]
16. Park JL, Shu L, Shayman JA. Differential involvement of COX1 and COX2 in the vasculopathy associated with the {alpha}-galactosidase A-knockout mouse. *Am J Physiol Heart Circ Physiol*. 2009; 296:H1133–H1140. [PubMed: 19202000]
17. Ariyaratna A, Palijan A, Dutil J, Prithiviraj K, Deng Y, Deng AY. Dissecting quantitative trait loci into opposite blood pressure effects on Dahl rat chromosome 8 by congenic strains. *J Hypertens*. 2004; 22:1495–1502. [PubMed: 15257171]



18. Saad Y, Yerga-Woolwine S, Saikumar J, Farms P, Manickavasagam E, Toland EJ, Joe B. Congenic interval mapping of RNO10 reveals a complex cluster of closely-linked genetic determinants of blood pressure. *Hypertension*. 2007; 50:891–898. [PubMed: 17893371]
19. Crissman RS, Guilford W. The three-dimensional architecture of the elastic-fiber network in canine hepatic portal system. *Am J Anat*. 1984; 171:401–413. [PubMed: 6517039]
20. Sarzani R, Brecher P, Chobanian AV. Growth factor expression in aorta of normotensive and hypertensive rats. *J Clin Invest*. 1989; 83:1404–1408. [PubMed: 2703537]
21. Wilcox JN, Smith KM, Williams LT, Schwartz SM, Gordon D. Platelet-derived growth factor mRNA detection in human atherosclerotic plaques by in situ hybridization. *J Clin Invest*. 1988; 82:1134–1143. [PubMed: 2843568]
22. Cines DB, Pollak ES, Buck CA, Loscalzo J, Zimmerman GA, McEver RP, Pober JS, Wick TM, Konkle BA, Schwartz BS, Barnathan ES, McCrae KR, Hug BA, Schmidt AM, Stern DM. Endothelial Cells in Physiology and in the Pathophysiology of Vascular Disorders. *Blood*. 1998; 91:3527–3561. [PubMed: 9572988]

### Perspectives

Identification of the genes governing neointimal hyperplasia and vascular reactivity could have a major impact on the effective treatment of cardiovascular diseases with angioplasty, bypass and endarterectomy of the peripheral and coronary vessels. Although a lot is known about the development of NIH as a result of vascular injury to the endothelium<sup>1, 19-22</sup>, the cause-effect relationships between vessel occlusion and vascular reactivity remain unexplored. In this context, our study is unique because isolation of the RNO3 interval associated with differences in NIH and vascular reactivity in the SHR.BN3 congenic strain can now be used to 1) assess relationships between NIH and vascular reactivity, 2) discern whether these are independent or associated phenotypes and 3) design and develop new therapies to prevent vascular restenosis following invasive vascular procedures.

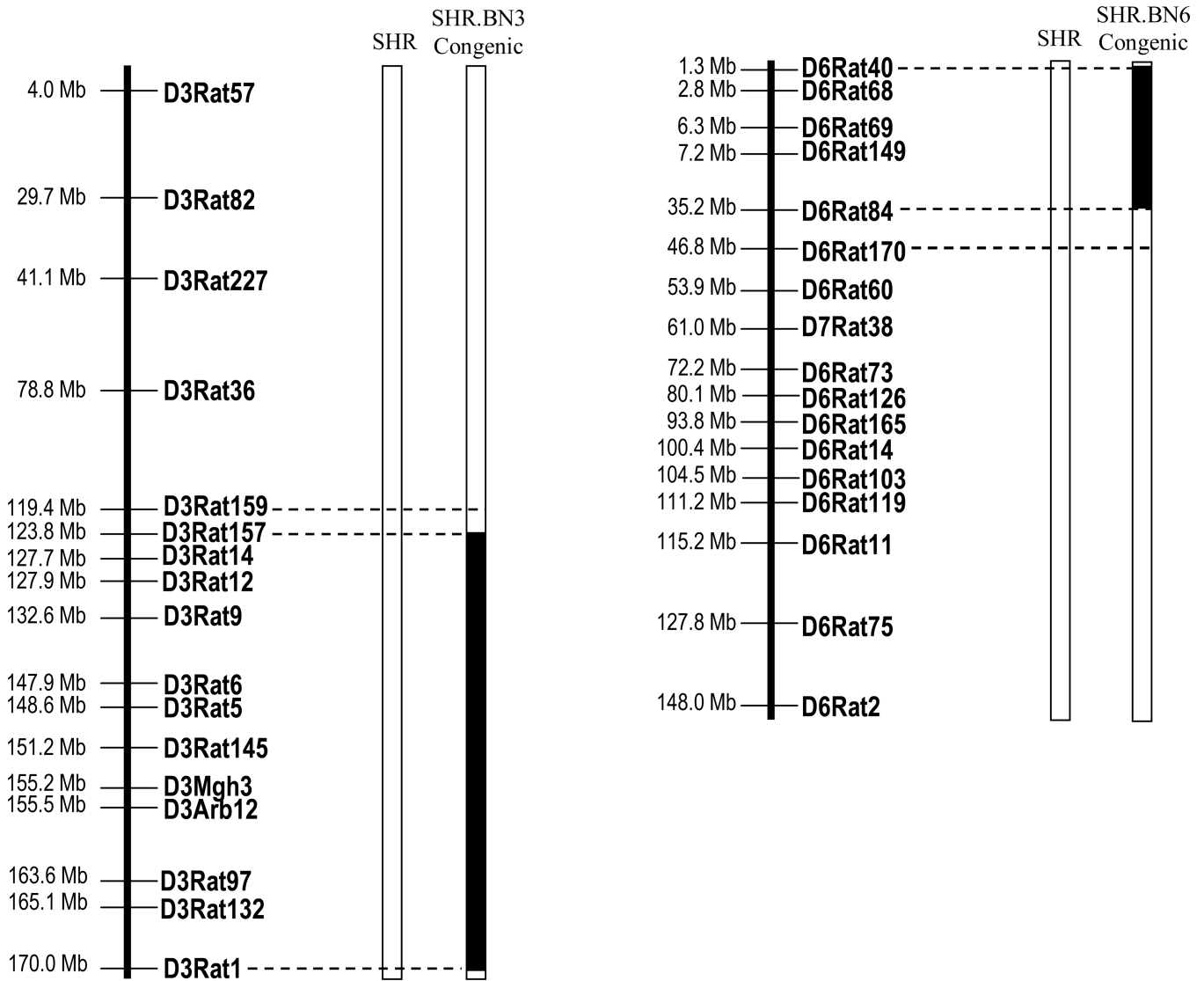


**Figure 1.** Physical maps of the congenic intervals. Parental strains are represented as open bars. Solid bars illustrate the BN segment introgressed onto the background of the SHR in congenic strains. Open bars at the end of each introgressed segment between dashed lines represent the regions of recombination. Markers outside the congenic region were genotyped and considered to be SHR alleles. The markers *D3Rat1* and *D6Rat40* are the markers genotyped at the ends of chromosomes 3 and 6, respectively. Mb = Megabases, *D7Rat38* is a marker on RNO6 ([www.rgd.mcw.edu](http://www.rgd.mcw.edu)).

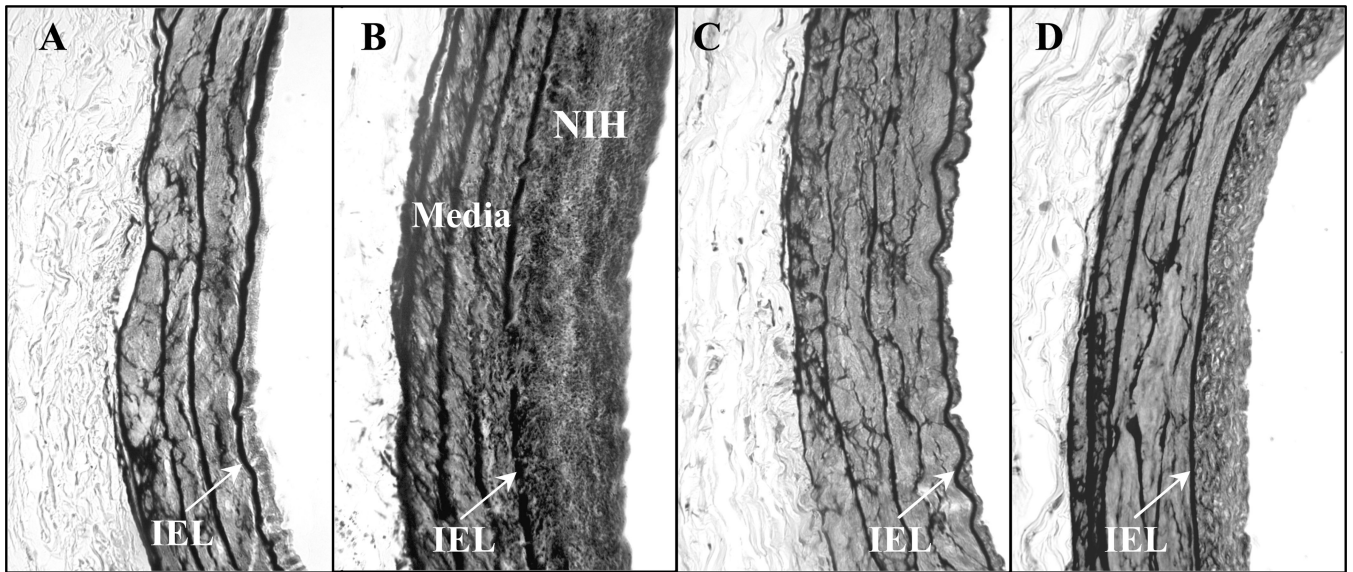
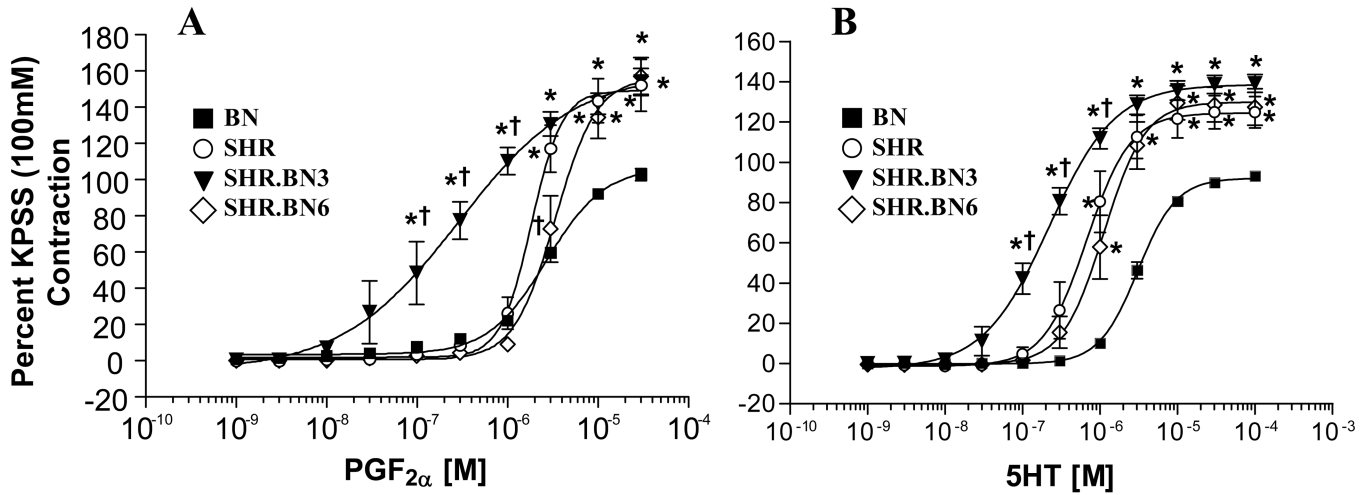


**Figure 2.**

Representative images of NIH formation in the left iliac arteries of the (A) SHR, (B) SHR.BN3, (C) SHR.BN6 and (D) SHR.BN (3 +6) strains 8 weeks post-injury. Vessels were formalin-fixed paraffin-embedded sections stained with Verhoeff-Van Gieson for elastin (40× magnification). IEL, Internal elastic lamina.



Strain	-log EC <sub>50</sub> [M]	
	PGF <sub>2α</sub>	5HT
BN	5.57 ± 0.03 (3)	5.51 ± 0.02 (3)
SHR	5.74 ± 0.04 (3)	6.17 ± 0.07 (3)*
SHR.BN3	6.54 ± 0.14 (3)*†	6.66 ± 0.05 (3)* †
SHR.BN6	5.47 ± 0.05 (3)	5.95 ± 0.06 (3)*

Data are expressed as mean ± SEM for number of animals in parentheses.

\* =  $p < 0.05$  compared to BN by one-way ANOVA followed by Bonferroni post-hoc test.

† =  $p < 0.05$  compared to SHR by one-way ANOVA followed by Bonferroni post-hoc test.

**Figure 3.**

Vascular reactivity experiments of endothelium denuded carotid artery rings of the SHR and BN parental strains and the SHR.BN3 and SHR.BN6 congenic strains. Concentration response curves for the agonists (A) Prostaglandin F<sub>2α</sub> (PGF<sub>2α</sub>) and (B) Serotonin (5HT). (C) Potency of agonists (-log EC<sub>50</sub>) in carotid artery rings for each strain.

\* =  $p < 0.05$  compared to BN by one-way ANOVA followed by Bonferroni post-hoc test.

† =  $p < 0.05$  compared to SHR by one-way ANOVA followed by Bonferroni post-hoc test.

Table 1

Comparison of the injured vessel parameters measured for the parental SHR, SHR.BN3 and SHR.BN6 congenic strains.

Parameter	N	%NIH	NIH Area mm <sup>2</sup>	Circular Area mm <sup>2</sup>	Media Area mm <sup>2</sup>	Media Width mm <sup>2</sup>	Lumen Size mm <sup>2</sup>
SHR Inj.	20	9.63 ± 90 <sup>‡</sup>	0.0125 ± 100 <sup>‡</sup>	0.3824 ± 17 <sup>‡</sup>	0.1020 ± 20	0.0438 ± 16	0.3699 ± 16 <sup>‡</sup>
SHR.BN3 Inj.	13	28.31 ± 67 <sup>**‡</sup>	0.0377 ± 77 <sup>**‡</sup>	0.3899 ± 31	0.0846 ± 33 <sup>**‡</sup>	0.0378 ± 43	0.3522 ± 32
SHR.BN6 Inj.	25	12.60 ± 72 <sup>‡</sup>	0.0172 ± 80 <sup>‡</sup>	0.4507 ± 17 <sup>*</sup>	0.1120 ± 18 <sup>‡</sup>	0.0446 ± 17	0.4335 ± 17 <sup>*</sup>

Data are expressed as the mean ± %CV.

\* Differ  $p < 0.01$  vs. SHR by one-way ANOVA.

<sup>‡</sup> Differ  $p < 0.01$  vs. SHR.BN3 by one-way ANOVA.

<sup>‡</sup> Differ  $p < 0.01$  vs. SHR.BN6 by one-way ANOVA.

**Table 2**

Comparison of the uninjured contralateral control vessel parameters measured in the parental SHR, SHR.BN3 and SHR.BN6 congenic strains.

Strain	N	Circular Area mm <sup>2</sup>	Media Area mm <sup>2</sup>	Media Width mm <sup>2</sup>	Body-weight adj heart-weight <sup>§</sup> mg/g
SHR	17	0.4479 ± 21	0.1218 ± 20	0.0483 ± 14	1272 ± 6
SHR.BN3	13	0.3937 ± 28 <sup>‡</sup>	0.1008 ± 46 <sup>‡</sup>	0.0418 ± 28 <sup>‡</sup>	1402 ± 12
SHR.BN6	25	0.4977 ± 21 <sup>‡</sup>	0.1396 ± 22 <sup>‡</sup>	0.0524 ± 17 <sup>‡</sup>	1303 ± 5

Data are expressed as the mean ± %CV.

\* Differ  $p < 0.01$  vs. SHR by one-way ANOVA.

<sup>‡</sup> Differ  $p < 0.01$  vs. SHR.BN3 by one-way ANOVA.

<sup>‡</sup> Differ  $p < 0.01$  vs. SHR.BN6 by one-way ANOVA

<sup>§</sup> Body-weight adjusted heart-weight calculated adjusting heart-weight for differences in body-weight using the regression of heart-weight on body-weight.